EXPERIMENTAL AND NUMERICAL DYNAMIC ANALYSIS OF PLEXIGLASS ACRYLIC FOR IMPACT ENERGY USING INDIGENOUSLY DEVELOPED TESTING EQUIPMENT

Tariq JAMIL [11*], Kashif AZHER[1], Muhammad Ali TAHIR[1], Zaheer ALI[1], Wassam HAMEED[1], Hafiz Huzefa JAVED[1]

Toughness, also known as impact energy, should be determined for any material that is under the action of impact loading. The fabrication of impact tester and dynamic analysis of fracture will be very helpful for various materials. In this study, an Izod impact testing equipment is designed and fabricated from scratch and demonstrated. It is utilized for determining the impact energy of Plexiglass Acrylic following ASTM D-256 standard. The designed equipment was well calibrated before performing experiments. The frictional and windage losses were also calculated without placing the sample to compensate for any error. The angles observed before and after the impact were utilized to calculate the impact energy of specimens. On ANSYS, the Finite Element Analysis and explicit dynamic analysis of the specimen were also investigated. The real-time deformation of the specimen after impact was observed. The stress and strain along the length of the specimen were investigated till the notch area. The analysis revealed that the maximum stress and strain at the notch due to the fracture point of the specimen. Hence, dynamic analysis validates the accuracy of the designed impact testing procedure.

Keywords: Impact Testing, Plexiglass, Indigenous, Izod test, Toughness

1. Introduction

There are various types of techniques widely utilized for materials testing such as tensile, compressive, impact, hardness, etc. It is mainly divided into two main types that are destructive and non-destructive testing. The selection of the material testing method depends upon the application of the material. The purpose of impact testing is to determine the ability of the material to absorb energy during a collision. The impact energy can be used to determine the toughness, impact strength, impact fracture resistance of the material [1]. The material characteristics can also be determined using impact testing. The determination of impact energy is also important for the selection of materials that are under the influence of sudden changes in loading conditions [2], [3].

For a single impact test, the three most popular types of tests are the Charpy V-notch test [4], [5], the Izod test [6] and the Tensile Impact test [7]. These three tests all essentially determine the same characteristics of the material but differ in the orientation of the test sample. All of these tests are useful in determining the impact mechanics of the test specimen.

[1] Asssistent Prof., NED University of Engineering and Technology, Pakistan, e-mail: tariqjamil@neduet.edu.pk

Various materials can be tested from impact loading, but the most common types used are metals [5], plastics [6], [8] and its composites [2], [9], and polymers [10]. All these tests have prescribed dimensions of specimens that can evaluate. Some composite or other specific materials could experience either ductile or brittle failure depending on the type of test, rate of loading, and temperature of the sample. The combined effect of ductile and brittle fracture was observed in the chemical mechanical planarization of silicon wafers [11]. Brittle material can fracture at low impact velocity and the amount of energy to cause a fracture is also small. On the other hand, ductile materials can fracture at relatively high impact velocities and at a much higher load to initiate and propagate the crack to fracture [12].
Among the above-mentioned impact testing, Izod impact testing is utilized for various materials [13], [14], [15]. The Izod impact testing was successfully utilized to examine the impact strength of acrylic denture base resin reinforced with woven glass fiber. The impact testing was utilized to observe the effect of the orientation of reinforced woven glass fibers [16]. The Izod testing was also utilized to examine the impact toughness of carbon fiber reinforced plastics for variable notch dimensions. It was also observed that the impact toughness rises with the fiber proportions [6]. Izod testing was found effective for the specimens that were prepared using 3D printing [17]. Different types of composites, polymers impact strength were also successfully observed using Izod testing technique [18].

An impact testing equipment was utilized to calculate the amount of impact energy or toughness of a material. Generally, the hammer and pendulum setup was utilized to calculate the amount of energy. The specimen was prepared as per the standard of the material. The impact testing machine was fabricated and utilized for various materials [13], [19].

There are various polymer materials and they possess various benefits in the field of medicines, composite materials, etc. [20] The polymers were also utilized for the drug delivery system which revolutionized the biomedicine world [21]. When the World Health Organization declared COVID-19 a pandemic, CDC and OSHA recommended the use of barriers such as Plexiglass, strip curtains, or similar impermeable dividers to separate manufacturing workers or meat and poultry processing workers [22]–[25]. Polymer impact testing was also widely studied. Rafique [26] fabricated equipment for the impact testing of polymer thin films by the free-falling dart method. Various studies have investigated the fracture toughness of plexiglass acrylic [27], [28]. These studies have thoroughly investigated the fracture toughness of different modes of testing based on Plexiglass structures.

In this study, we have performed an Izod type Impact testing on the plastic specimen that is Plexiglass Acrylic, experimentally as per the standard of ASTM D256 [29]. Along with the experiment, we have fabricated the Izod impact testing equipment. The complete 3D model of the impact testing equipment was designed

using computer-aided designing software. The specimens of Plexiglass were also fabricated as per the standard. Moreover, FEA-based dynamic analysis was also performed to elaborate on the results. Both the FEA and dynamic analysis was performed using the same specification as that of specimens on ANSYS software. The novelty and value addition of this article has two aspects. The first is the cost-effective in-house fabrication of laboratory equipment, which can save huge capital. The second aspect of this article as this study validates the experimental results with numerical analysis. So similar accurate approach can also be applied to various other materials in future studies.

2. Materials and Methods

2.1 Design of Impact Testing Equipment

In our design of the impact testing equipment, a specimen was fixed in a vise which is placed on top of a stainless steel base. A pendulum striker was elevated and then released from a certain height above the specimen. The striker hits the specimen with an impact speed that depends on the height from where it is dropped. The kinetic energy of the striker was then absorbed by the specimen, which reduced the kinetic energy of the pendulum.

The design of impact testing equipment as per the standards of ASTM D256 started with the 2D sketch of the base and columns. The dimensions of the base and columns that are 40 × 60 cm and 20 × 0.6 cm respectively, were designed in accordance with ASTM D256. The columns were fastened to the base, and the geometry of a vise was assembled at the centre of two columns. After that, the geometry of specimen materials was designed whose dimensions could not be violated by the standards. The specimen of cross-section 1.27 × 1.27 cm and a length of 6 cm along with a notch of 0.25 cm at the center was created and held inside the vise. The material of the specimen and impact testing equipment are made up of Plexiglass Acrylic and stainless steel, respectively. Fig. 1a depicts the final 3D design of the project after assembly, which shows the isometric views of an impact testing machine designed using CAD 3D modeling software in accordance with the ASTM D-256 standard. The final model of the project after the assembly is as shown in Fig. 1b.

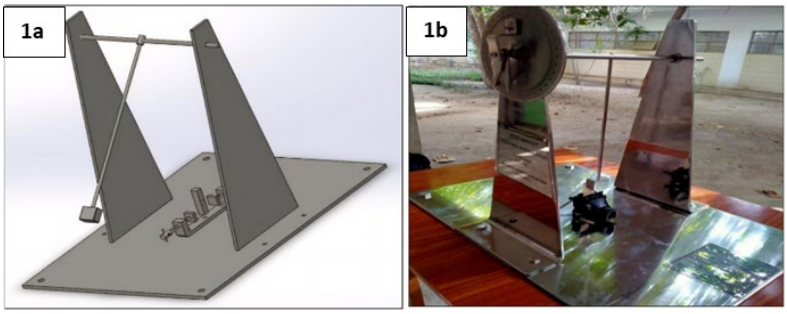

Fig. 1 **a** CAD model of Impact Testing machine designed by following ASTM D-256 standards and **b** shows the impact testing apparatus after fabrication. It is made using stainless steel of grade HS-304 Taiwan

2.2 Fabrication and Assembly

The whole fabrication process consists of four steps, fabrication of the base and columns, fabrication of the pendulum and hammer, fabrication of the dial and pointer, and final assembly. The mainframe of equipment consists of two vertical columns mounted on a single base. The columns are fastened to the base using nuts and bolts. 4 holes were drilled on top of the base to mount it on a wooden table. The cross-sectional area of the base is 60 × 40 cm and the thickness is 0.6 cm, whereas, the column has the same thickness but with a length of 50 cm. The pendulum and hammer are utilized to observe any material's impact energy by striking it with the specimen. In Izod type impact testing of plastics and polymers, the hammer strikes the specimen with the velocity of 3.46 m·s-1. In accordance with the standards, the length of the pendulum used is 0.33 m and the weight is 260 gm. A dial was made up of a 6 mm thick circular stainless steel disk and calibrated with reference of angles in degrees using the etching process. The pointer attached indicates the value of the angle at which the specimen breaks. Impact energy can be calculated using the impact angle observed.

2.3 Specimen Preparation and Conditioning

The specimens were cut from the material sheet as per prescribed dimensions. The width of the as prepared specimen is the same as the thickness of the sheet that is 12.7 mm [0.500 in]. Sheet material thicker than 12.7 mm should be machined to standard dimensions. Specimens with a 12.7 mm square cross section were used for testing. The test specimen shall be a composite of individual thin specimens ranging in width from 6.35 to 12.7 mm [0.250 to 0.500 in]. The length of the specimen under the notch was 10.16 ± 0.05 mm [0.400 ± 0.002 in.]. This dimension was measured with a Vernier caliper. The labelled 2D sketch of the specimen is shown in Fig. 2a. The notch on the specimen was made using a milling machine and a single-tooth cutter was preferred due to ease of operation. A work

relief angle of 15 to 20° is suitable. The included angle of the notch is 45° and the radius of curvature at the apex is 0.25 mm while the depth of the notch should be maintained to 3 mm. A dummy bar was placed behind the specimen in the vise to prevent distortion and chipping by the cutter. Cutter's speed and feed rate should be set precisely because they could affect the quality of the notch due to thermal deformations and stresses. The 3D CAD model of the specimen is presented in Fig. 2b.

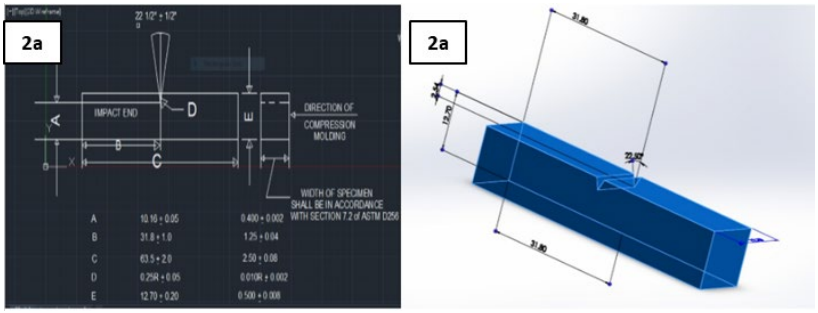

Fig. 2 **a** Shows the 2D view of the Plexiglass specimen made using AUTOCAD software with labelled dimensions of the specimen and **b** represents the 3D model of the notched specimen

The most suitable testing temperature of the specimen is 25°C. The shorter conditioning time would be beneficial in order to achieve impact resistance equilibrium. The relative humidity tolerance should be from 45% to 55%. At the maximum surrounding temperature of 25°C, the maximum humidity would be 55%. In case of deviation, temperature tolerance should be less than or equal to 1°C and relative humidity should be more or less 2%.

2.4 Center of percussion

The point (line) of contact of the cylindrical striker must be located at the center of percussion of the pendulum within ±2.54 mm [±0.100 in] in order to minimize the vibrations produced when the striker hits the specimen. The distance from the center of percussion to the axis of support was determined experimentally from the period of small amplitude oscillations of the pendulum by means of the following equation:

$$L = \left({}^{g}/_{4\pi^2}\right) p^2$$

The angle of each swing should be less than 5° on each side of the center as mentioned in standard. Where, g is local gravitational acceleration m·s^{-2} or [ft·s^{-2}], L is distance from the center of percussion to the axis of support, m or [ft.], and p is period (sec) of a single complete swing (to and fro) determined by taking mean at least 20 successive and continuous swings.

From Table 1, the center of percussion for pendulum in this study is found to be 0.3244 m [1.02 ft.]. Therefore, the length of the percussion centre subtracted from the pendulum's total length gives 0.005 m [0.016 ft.] which is under the prescribed limit. This resulted in the least amount of vibrational energy loss when the striker

hit the specimen from this point of percussion. Thus, our pendulum has the same center of percussion and center of gravity: the length of the pendulum or distance from the center of percussion to the axis of support = 0.33 m.

Table 1

Shows the values obtained to calculate the center of percussion of the pendulum striker

Serial. No	P_{20} (s)	P_1 (s)	$L = \left(g/4\pi^2\right) p^2$ (m)
1	23.2	1.16	0.3244
2	22.8	1.14	
3	22.6	1.13	

2.5 Experimental Testing Procedure

The test was performed five times on 10 specimens. The average of the results of the test was evaluated as final impact toughness. The pendulum was raised at an angle 60° above the horizontal, making the total angle of 150° and the height of release is 0.61m. This height and pendulum mass of 260 gm produce an impact speed of 3.46 m·s-1 First, the pendulum was released at 150° without holding the specimen in vise to calculate the windage and friction factor of the testing apparatus. Then specimens were clamped in the vise one by one, the upper half till the notch was above the jaws of the vise and the pendulum was released at 150°. The angles obtained after the specimen were observed and used to calculate the impact energy.

3. Result and discussion.

3.1 Observation and Calculation

The pendulum was released at an angle of 150° (60° above the horizontal) and the angle obtained after the striker of the pendulum hit the specimen was observed 105° (15° above horizontal axis) which resulted in the breakage of the specimen. 10 specimens were tested at 150° and various angles between 105° to 110° were observed. Table 2, depicts the impact energy observed for all the samples along with the difference between the heights.

Table 2

Following is the observation and calculation table for all the specimens

S.No.	Observation (Scale reading) (°)	$h_2 = L - L \times \cos\theta$ (m)	$h = h_1 - h_2$ (m)	$E_s = m \times g \times h$ (J)
1	105	0.4154	0.1946	0.49
2	108	0.4319	0.1781	0.45
3	109	0.4374	0.1726	0.43
4	107	0.4264	0.1836	0.46
5	105	0.4154	0.1946	0.49
6	107	0.4264	0.1836	0.46
7	108	0.4319	0.1781	0.45
8	106	0.4209	0.1831	0.46

9	107	0.4264	0.1836	0.46
10	110	0.4428	0.1672	0.42

So, $$Angle = \theta = 105°$$

Since the height of the pendulum when it is raised to 150° is:

$$h_1 = 0.61\ m \quad (1)$$

Also, the height of the pendulum after striking the specimen can be obtained by taking the cosine component of the effective length of the pendulum that is 0.33 m.

$$h_2 = L - L \times cos\,\theta = 0.33 - (0.33 \times cos(105°)) = \mathbf{0.4154\ m} \quad (2)$$

Where, L= length of a pendulum

Now, the difference between the heights of the pendulum can be obtained by simply subtracting h_2 (height achieved after breaking the specimen) from h_1 (releasing height of pendulum). So,

$$h = h_1 - h_2 = 0.61 - 0.4154 = \mathbf{0.1948\ m} \quad (3)$$

Now, the total impact energy in joules can be obtained by using the formula:

$$E_s = m \times g \times h = 0.260 \times 9.8 \times 0.1948 \quad (4)$$

$$E_s = 0.4963\ J \quad (5)$$

Where, m= mass of pendulum, which is 260 g

g = Gravitational acceleration constant =9.8 $m \cdot s^{-2}$

E_s = Uncorrected breaking Energy / dial reading breaking Energy for the specimen (J)

L = length of pendulum (distance from fulcrum to center of gravity of pendulum)

The testing equipment used a dial and pointer mechanism. Therefore, it is necessary to calculate the windage and friction correction factor for our result in order to facilitate the losses in our result. The friction and windage factor was calculated using the method mentioned in section 10 and with Annexure A2 and Appendix X3 of ASTM D-256 [29].

Table 3, shows the calculated results for losses and standard deviation of our performed experiment. Measure and record the energy correction (E_A) for windage of the pendulum plus friction in the dial, as determined with the first swing of the pendulum with no specimen in the testing device. This correction must be read on the energy scale appropriate for the pendulum used. Without resetting the position of the indicator, repeat the process until the swing causes no additional movement, measure the energy correction (E_B) or pendulum windage. The following results were obtained

The angles obtained were $\theta_A = 138°$ and $\theta_B = 142°$

Table 3

Shows the final result after calculating friction and windage losses, mean 10 specimens result, and standard population deviation that could occur in the result

Sr. No	$E_s = m \times g \times h$ (J)	β (°)	E_{TC} (J)	I_s (J/m)	Mean of 10 Specimens (J/m)	Standard Deviation[S.D]
1	0.49	105.18	0.0735	32.79	30.107	1.707191
2	0.45	108.04	0.0748	29.54		
3	0.43	109.49	0.0755	27.91		
4	0.46	107.32	0.0745	30.35		
5	0.49	105.18	0.0735	32.79		
6	0.46	107.32	0.0745	30.35		
7	0.45	108.04	0.0748	29.54		
8	0.46	107.32	0.0745	30.35		
9	0.46	107.32	0. 0745	30.35		
10	0.42	110.22	0.0748	27.10		

$E_A = 0.0885\,J$ [Energy correction for windage of pendulum plus dial (J)]
$E_B = 0.0508\,J$ [Energy correction for pendulum windage only (J)]
$E_M = 1.555\,J$ [Max Energy of the pendulum at start of the test (J) (at release point of 60° above horizontal/0.61m release height)]

$$\beta_{max} = cos^{-1}\{1 - [\,(\frac{h_1}{L})(1 - \frac{E_A}{E_M})]\} = 138.00° \quad (6)$$

Where,
h_1 = maximum height of the center of gravity of the pendulum (0.61 m)
β_{max}= maximum angle pendulum will travel with one swing of the pendulum.
Now calculating β and E_{TC} for each specimen using obtained E_s (J)

$$\beta = cos^{-1}\{1 - [\,(\frac{h_1}{L})(1 - \frac{E_s}{E_M})]\} \quad (7)$$

$$E_{TC} = \left[E_A - \left(\frac{E_B}{2}\right)\right]\left(\frac{\beta}{\beta_{max}}\right) + (\frac{E_B}{2}) \quad (8)$$

$$I_s = (E_s - E_{TC})/t \quad (9)$$

Where,
L = length of the pendulum (distance from the fulcrum to center of gravity of pendulum,) = 0.33m,
β = angle pendulum travels for a given specimen,
E_{TC} = total correction energy for the breaking energy, Es, of a specimen (J)
I_S = impact resistance of specimen, $J{\cdot}m^{-1}$ [$ft.lbf{\cdot}/in^{-1}$] of width, and
t= width of specimen in m [in] = 0.0127m.
Range (lower limit) = $[mean - 3 * S.D]$ =24.94
Range (Upper limit) = $[mean + 3 * S.D]$ =35.22

According to the mean and standard deviation, we can say that the results for this specific specimen will only deviate from 24.94 $J{\cdot}m^{-1}$ to 35.22 $J{\cdot}m^{-1}$. Other authors also report these variations in results [30], [31]. The specimen tested was

isotropic and the complete splitting of the specimen occurred (ASTM D-256 Type C break; in which the specimen completely breaks into two parts). The fracture occurred at the notch and propagated along the line of impact. The specimen before and after fracturing is presented in Fig. 3 a and b, respectively. The failure of the specimen is similar to brittle fracture as no elongation was observed during the fracture of the specimen [32].

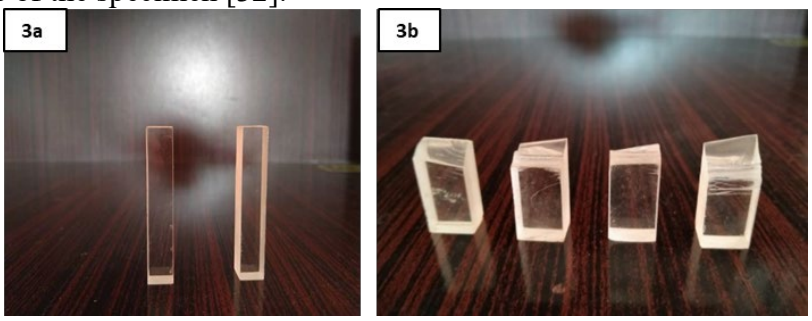

Fig. 3 **a** Shows specimen's sample before making a notch and **b** shows the fractured specimen after being impacted using a pendulum striker. It is a type C fracture in which material completely breaks off into two pieces.

3.2 FEA and Explicit Dynamic Analysis

First, to investigate the dynamic analysis of impact testing, we perform finite element analysis (FEA). The numerical modeling of other polymers was studied previously using different impact testing technique [33]. Considering the dynamic analysis, splitting of the specimen results when the striker of the pendulum applies dynamic impact load and velocity onto the specimen. Whereas, FEA includes the meshing of both the specimen and the striker. The whole process of dynamic analysis is done in the following steps.

The first step of dynamic analysis is the selection of material and its data. The material selected for the specimen is Plexiglass and the striker is hardened steel. We input the values of density (1180 kg.m^{-3}), Young's modulus (3.1026E+009 Pa), and Poisson ratio (0.35) for the specimen. We also input the values of density, Young's modulus and Poisson ratio for the striker. ANSYS provided us with the values of bulk modulus and shear modulus while the temperature and other experimental conditions were maintained as prescribed above.

The geometry of both the specimen and the striker is created as per the dimensions of the specimen are $(1.27 \times 1.27 \times 6)$ cm and of the striker are $(3.47 \times 7.2 \times 2)$ cm. Meshing was performed on both the specimen as well as the striker. There was a total of 7649 nodes and 6176 elements (specimen: 2736 nodes and 2080 elements, striker: 4913 nodes and 4096 elements). In this step, the specimen is clamped below the notch, and the striker is provided with a velocity of 3.46 m·s^{-1} as per the standard. The maximum number of cycles is kept at $1E+7$, and the end time was 0.01s. The deformation caused by the striker is shown in Fig. 4. In line with the experimental results, the specimen is broken from the center

where the notch is present. No significant deformation is observed as the bottom part is fixed with the base using a clamp, and the significant deformation is above the notch.

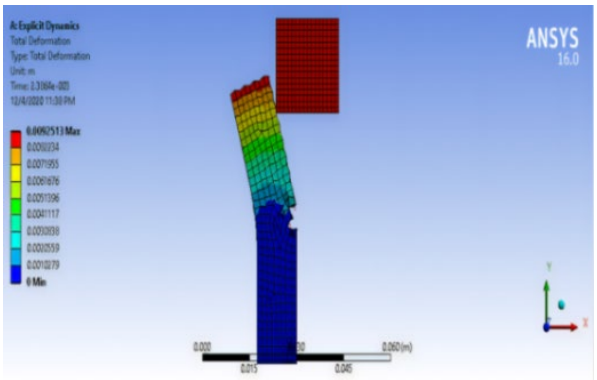

Fig. 4 Represents the results obtained after performing dynamic analysis using ANSYS software, all the conditions were kept similar to experimental conditions.

3.3 Total Deformation

Table 4, depicts the deformation values of the specimen obtained through explicit dynamics analysis in relation to the impact of the testing experiment. The pictorial view shown in Fig. 4, represents the maximum deformation produced at the top of the specimen. The values in Table 4, are then plotted with time as shown in Fig. 5a. The color scheme shown in Fig. 4 explains the deformation produced by the striker. Fig.5b shows the deformation along with the specimen from top to the notch which is being impacted. The maximum deformation was observed at the top and decreases as we move along the length, but at the notch, there is a spike in the graph. This rise in deformation is due to a decrease in the area of the specimen at the notch.

Table 4

Shows the result of total deformation produced by impact force with the help of ANSYS simulations

Time (s)	Minimum (m)	Maximum (m)
1.18 E-38	0	0
5.00 E-04		1.82 E-03
1.00 E-03		3.64 E-03
1.50 E-03		5.46 E-03
2.00 E-03		7.30 E-03
2.39 E-03		9.25 E-03

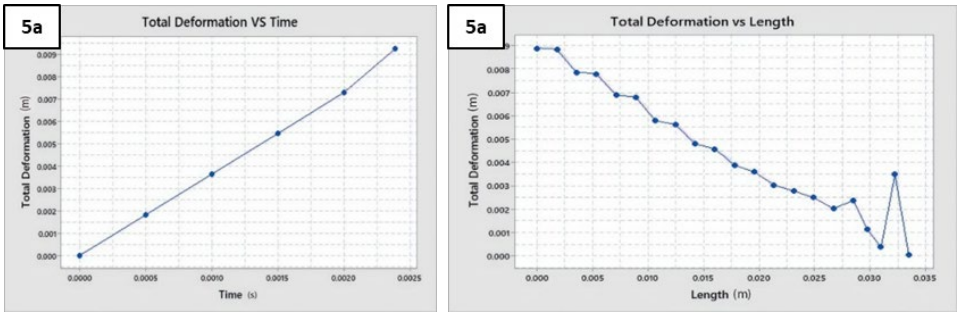

Fig. 5 **a** Shows the graphical representation of total deformation produced in the specimen and the time in which it is produced, and **b** graph represents the total deformation produced along the length of the specimen, from stating the length of 0.00 mm to the notch at 0.035 mm.

3.4 Equivalent Elastic Strain

Fig. 6 represents the strain produced in the specimen under impact loading and it is maximum at the notch due to an increase in stress concentration. The breakage of the specimen is from the notch in a numerical analysis similar to experimental observation. Fig. 7a represents the linear trend of time (short impact time) with the elastic strain. Elastic strain at the top and bottom of the specimen is zero and maximum at the centre. Fig. 7b shows the elastic strain along the length of the specimen which is being impacted from top to the center of the specimen. It can be observed that no strain was produced at the top and the strain increases are also small along the length. Whereas at the notch, there is a sudden increase in the graph which shows the maximum elastic strain occurs at the notch, which is the fracture point of the specimen. The tabular results are obtained using explicit dynamics analysis shown in Table 5.

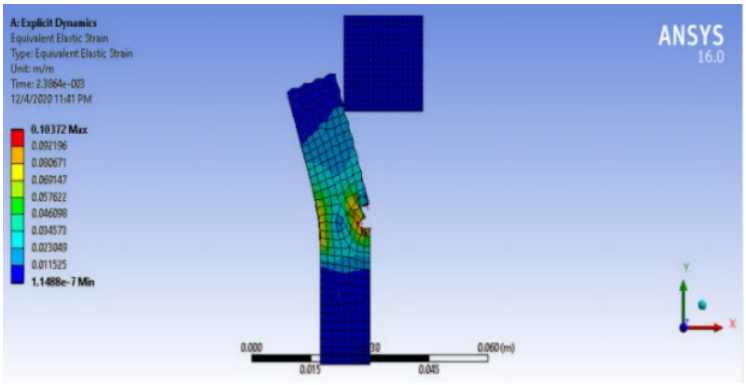

Fig. 6 Represents the result of explicitly dynamic analysis, showing equivalent elastic strain produced in the specimen as a result of impact produced by a striking hammer, having a speed of 3.43 ms^{-1}.

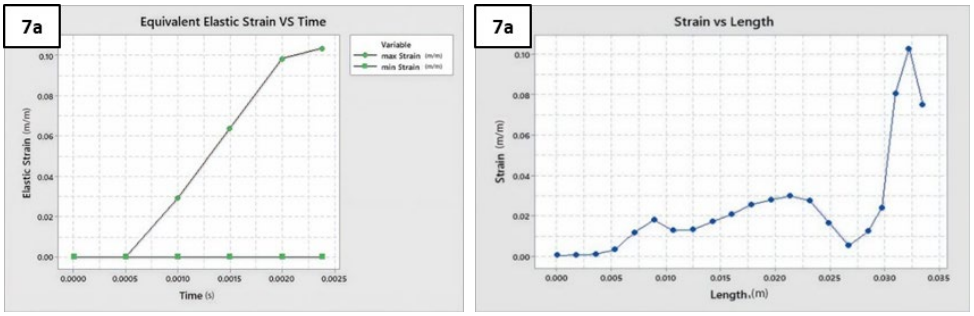

Fig. 7 **a** Shows the graphical representation of the tabular data presented in table 5, showing the values of maximum and minimum equivalent elastic strain. **b** Graph represents the equivalent elastic strain produced along the length of the specimen.

Table 5

Represents the result obtained by numerical analysis and also shows the values of maximum and minimum strain produced in the body

Time (s)	Minimum (m/m)	Maximum (m/m)
1.18 E-38	0	0
5.00 E-04		1.16 E-07
1.00 E-03	3.80 E-08	2.92 E-02
1.50 E-03	1.99 E -08	6.39 E-02
2.00 E-03	5.87 E-08	9.85 E-02
2.39 E-03	1.15 E-07	1.04 E-01

3.5 Equivalent Stress

As the pendulum striker hits the specimen, it produces strain in it due to the impact. According to Hook's law, stress is directly proportional to strain within the elastic limit and here the stress induced in the specimen is the reaction of applied impact force. The values of the stresses observed are presented in both tabular and graphical forms. Fig. 8 is the pictorial view of the stress produced in the specimen and it is maximum at the center due to stress concentration at the notched area. Fig. 9a represents the trend of time (short impact time) with the elastic stress. Fig. 9b shows the equivalent stress along the length of the specimen (from top to notch) which is being impacted via pendulum striker. From the top to the center of the specimen, it can be seen that no stress is generated at the top and that it gradually increases along the length until the notch. At the notch area, a sudden rise in stress can be observed and maximum stress is obtained at the fracture point of the specimen. The tabular results are obtained using explicit dynamics analysis shown in Table 6.

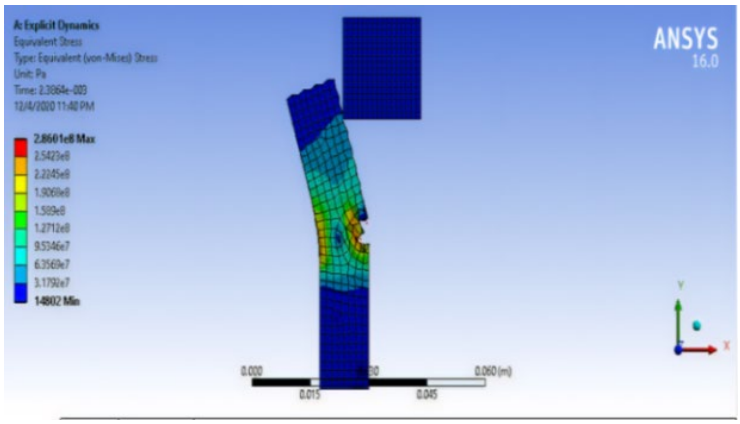

Fig. 8 Shows fracture occurring from the area of the notch, similar to the experimental results obtained in the first part of our study.

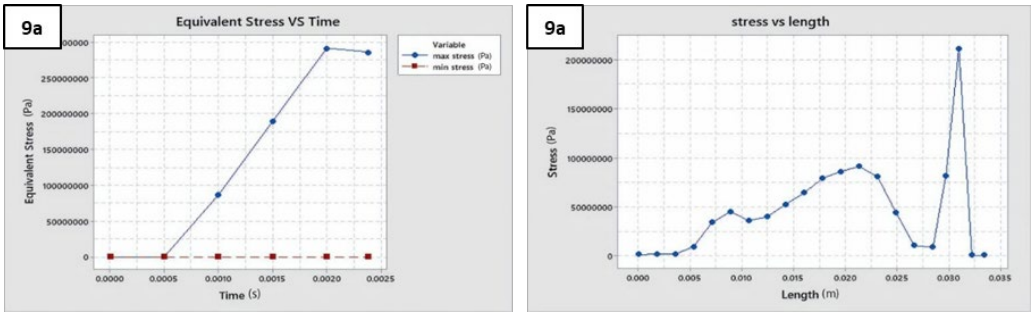

Fig. 9 **a** Graphical representation of the tabular data presented in table 6 and **b** Depicts the graphical representation of the equivalent stress produced along the length of the specimen.

Table 6

Shows the values of maximum and minimum stresses (Pa) produced internally

Time (s)	Minimum (Pa)	Maximum(Pa)
1.18 E-38	0	0
5.00 E-04		344.41
1.00 E-03	3002.8	8.66 E+07
1.50 E-03	1552.2	1.89 E+08
2.00 E-03	3901.8	2.92 E+08
2.39 E-03	14802.0	2.86 E+08

4. Conclusion

Analysis and testing are considered a vital task for performing the impact fracture testing of material. The impact testing, FEA, and dynamic analysis on Plexiglass material were performed in this study. The impact testing was performed on indigenously designed equipment. The equipment and specimens were designed as per the standard of ASTM D256. The specimen had fixed dimensions other than

the width that could be varied as per the standard. The base, column, pendulum, and striker were also designed as per the standard. All the testing was performed on Plexiglass material for 10 specimens. The impact testing for all the specimens was performed successfully and with complete breakage. The impact energy was calculated using the angles observed and taking an average of 10 specimens. The average impact energy value was found to be 30.1 J/m with a standard deviation of 1.7 J/m. The small deviation was obtained which proved the accuracy of the performed experiment. FEA and dynamic analysis were also performed. The results of the analysis indicate a successful impact fracture of the specimen. The intensity diagram, table, and graphs for deformation show that the maximum deformation was found at the top of the specimen and zero below the notch due to fixed in the vise. For stress and strain analysis, the results indicate that both the stress and strain are maximum at the notch since the stress concentration is increased due to the presence of the notch, which resulted in the fracture of the specimen.

REFERENCES

[1] *R. L. Bertoltti*, "Strength and Absorbed Energy in Instrumented Impact Tests of Polycrystalline Al2O3," Journal of the American Ceramic Society, **vol.** 57, no. 7, Jul. 1974, pp. 300–302

[2] *P. O. Sjoblom, J. T. Hartness, and T. M. Cordell*, "On Low-Velocity Impact Testing of Composite Materials," Journal of Composite Materials, **vol.** 22, no. 1, 1988, pp. 30–52

[3] *H. Wang, H. Zhou, Z. Huang, Y. Zhang, and X. Zhao*, "Constitutive modeling of polycarbonate over a wide range of strain rates and temperatures," Mechanics of Time-Dependent Materials, **vol.** 21, no. 1, Feb. 2017, pp. 97–117

[4] *D. J. Ayres*, "Dynamic plastic analysis of ductile fracture - the charpy specimen," International Journal of Fracture, **vol.** 12, no. 4, 1976, pp. 567–578

[5] *A. Waqas, X. Qin, J. Xiong, C. Zheng, and H. Wang*, "Analysis of ductile fracture obtained by charpy impact test of a steel structure created by robot-assisted GMAW-based additive manufacturing," Metals, **vol.** 9, no. 11, 2019, pp. 1–12

[6] *N. L. Hancox*, "Izod impact testing of carbon-fibre-reinforced plastics," Composites, **vol.** 2, no. 1, 1971, pp. 41–45

[7] *ASTM-D1822-13*, "Standard Test Method for Tensile-Impact Energy to Break Plastics and Electrical Insulating Materials," 2013

[8] *R. B. Seymour*, "The Role Of Fillers And Reinforcements In Plastics Technology," Polymer-Plastics Technology and Engineering, **vol.** 7, no. 1, 1976, pp. 49–79

[9] *A. M. S. Hamouda and M. S. J. Hashmi*, "Testing of composite materials at high rates of strain: Advances and challenges," Journal of Materials Processing Technology, **vol.** 300, no. 3–4, 1998, pp. 327–336

[10] *A. Söver, L. Frormann, and R. Kipscholl*, "High impact-testing machine for elastomers investigation under impact loads," Polymer Testing, **vol.** 28, no. 8, 2009, pp. 871–874

[11] *T. A. Ring, P. Feeney, D. Boldridge, J. Kasthurirangan, S. Li, and J. A. Dirksen*, "Brittle and Ductile Fracture Mechanics Analysis of Surface Damage Caused During CMP," Journal of The Electrochemical Society, **vol.** 154, no. 3, 2007, pp. H239–H248

[12] *R. C. Batra and M. H. Lear*, "Simulation of brittle and ductile fracture in an impact loaded prenotched plate," International Journal of Fracture, **vol.** 126, no. 2, 2004, pp. 179–203

[13] *S. E. Slavin and G. T. BESWICK*, "Instrumented lzod Impact Testing," Journal of Applied Polymer Science, **vol.** 49, no. 6, 1993, pp. 1065–1070

[14] *M. N. Silberstein*, "Mechanics of Notched Izod Impact Testing of Polycarbonate," 2005.
[15] *R. Seldén*, "Fracture energy measurements in polycarbonate and PMMA," Polymer Testing, **vol.** 7, no. 3, Jan. 1987, pp. 209–222
[16] *K. F. Takahito KANIE, Hiroyuki ARIKAWA and and S. BAN*, "Impact Woven Strength of Acrylic Glass Fiber Denture Base Resin Reinforced," Dental Materials Journal, **vol.** 22, no. 1, 2003, pp. 30–38
[17] *D. A. Roberson, A. R. Torrado Perez, C. M. Shemelya, A. Rivera, E. MacDonald, and R. B. Wicker*, "Comparison of stress concentrator fabrication for 3D printed polymeric izod impact test specimens," Additive Manufacturing, **vol.** 7, 2015, pp. 1–11
[18] *C. Scott, H. Ishlda, and F. H. J. Maurer*, "Infrared analysis and Izod impact testing of multicomponent polymer composites: polyethylene/ EP D M /filler systems," Journal of Materials Science, **vol.** 22, no. 11, 1987, pp. 3963–3973
[19] *P. V. Brown*, "Richardson Co, IMPACT TESTING MACHINE," US2755658A, 1956
[20] *H. Namazi*, "Polymers in our daily life," *BioImpacts*, **vol.** 7, no. 2. Tabriz University of Medical Sciences, 2017, pp. 73–74, 2017.
[21] *O. Pillai and R. Panchagnula*, "Polymers in Drug Delivery Omathanu Pillai and Ramesh Panchagnula," Current Opinion in Chemical Biology, **vol.** 5, no. 4, 2001, pp. 447–451
[22] *CDC*, "Guidance for Pharmacies," 2020. https://www.cdc.gov/coronavirus/2019-ncov/hcp/pharmacies.html
[23] *Osha*, "COVID-19 Guidance for Retail Pharmacies." [Online]. Available: www.osha.gov/coronavirus
[24] *B. D. Adkins, M. P. Crawford, M. M. Maglione, and N. S. Aguilera*, "Special Articles Barriers at the Scope Use of Acrylic Shields at the Microscope During the Pandemic," Archives of Pathology & Laboratory Medicine, **vol.** 145, no. 3, 2021,
[25] *M. L. Fischman and B. Baker*, "Guidance on the use of plexiglass barriers for workplaces for 'sneeze guard' drop," *American College of Occupational and Environmental Medicine (ACOEM)*, 2020. https://acoem.org/COVID-19-Resource-Center/COVID-19-Q-A-Forum/Could-you-provide-guidance-on-the-use-of-plexiglass-barriers-for-workplaces-for-sneeze-guard"-dropl.
[26] *M. M. A. Rafique*, "Design of an impact testing machine for polymer films by the free falling dart procedure," Materials Testing, **vol.** 57, no. 9, Sep. 2015, pp. 799–805
[27] *X. Ji, W. Shang, X. Zhang, and J. Chen*, "Optical experiment testing for fracture toughness of directional plexiglass along different directions," https://doi.org/10.1117/12.839066, **vol.** 7375, Aug. 2009, pp. 404–409
[28] *M. R. M. Aliha, A. Bahmani, and S. Akhondi*, "Mixed mode fracture toughness testing of PMMA with different three-point bend type specimens," European Journal of Mechanics - A/Solids, **vol.** 58, Jul. 2016, pp. 148–162
[29] *ASTMD256-10*, "Standard Test Methods for Determining the Izod Pendulum Impact Resistance of Plastics," *ASTM International, West Conshohocken, PA (2018)*, 2018.
[30] *O. Research et al.*, "Comparison of Impact Strength and Fracture Morphology of Different Heat Cure Denture Acrylic Resins: An In vitro Study," Journal of International Oral Health : JIOH, **vol.** 6, no. 5, Sep. 2014, p. 12 Accessed: Jun. 22, 2022. Available: /pmc/articles/PMC4229820/
[31] *S. Watanabe, Y. Ishida, D. Miura, T. Miyasaka, and A. Shinya*, "Development of a Weight-Drop Impact Testing Method for Dental Applications," Polymers, **vol.** 12, no. 12, Dec. 2020, pp. 1–13

[32] *F. Faot, L. H. V Panza, R. C. M. R. Garcia, and A. A. D. B. Cury*, "Impact and Flexural Strength, and Fracture Morphology of Acrylic Resins With Impact Modifiers," The Open Dentistry Journal, **vol.** 3, no. 1, 2009, pp. 137–143

[33] *T. Krausz, I. I. Ailinei, S. V. Galatanu, and L. Marsavina*, "Charpy impact properties and numerical modeling of polycarbonate composites," Material Design & Processing Communications, **vol.** 3, no. 4, Aug. 2021, p. e260